Pure & Appl. Chem., Vol. 57, No. 11, pp. 1627–1638, 1985.
Printed in Great Britain.
© 1985 IUPAC

X-ray scattering measurements of order in non-crystalline polymers

A.H. Windle

Department of Metallurgy and Materials Science
Pembroke Street, Cambridge CB2 3QZ, U.K.

Abstract - The paper summarises the methods by which Wide Angle X-Ray Scattering (WAXS) can be analysed to give information about local order in non-crystalline polymers. In the case of disordered materials (conventional polymer glasses or melts) there is no indication that the overall conformation is anything but random coil. However, there are several features of the WAXS pattern which demonstrate special local interchain correlations. The same approach is also applied to WAXS of thermotropic liquid crystalline polymers. Polymers which feature in the examples described are: atactic, quenched isotactic and quenched syndiotactic PMMA; atactic polystyrene; polycarbonate and a thermotropic random copolyester based on hydroxy benzoic and hydroxy naphthoic acids.

INTRODUCTION

Diffraction techniques are preeminent in the study of molecular organisation in condensed phases. Wide angle X-ray scattering (WAXS) methods form the basis of X-ray crystallography, and yet their application to polymer melts and glasses has received less attention. However, the twin issues of chain conformation and local interchain correlations require information in the 1-50Å range where WAXS is particularly appropriate. Historically, some of the reluctance to apply WAXS techniques to the non-crystalline polymers appears to stem from difficulties in RDF analysis and even in believing that two or perhaps three diffuse haloes can actually contain much structural information!

WAXS procedures have provided direct experimental confirmation of accepted models of non-crystalline polymers and of conformational calculations. There have also been some structural surprises particularly in regard to polymers containing aromatic groups, and recently in the field of mesomorphic polymers.

This paper sets out to review the WAXS method using as a particular example PMMA, which might be seen as a fairly typical polymer glass. Attention is then turned to polystyrene, and other polymers such as polycarbonate with aromatic groups in the backbone. Finally, the scattering from thermotropic random copolyesters is discussed.

PMMA (i) RADIAL DISTRIBUTION FUNCTION (RDF) ANALYSIS

As one might expect, the scattering from PMMA is diffuse. A typical transmission diffractometer scan is shown in Fig. 1. Three broad maxima are apparent. The recasting of these data in real space to give the RDF is achieved by a Fourier Transform relation of the type:

$$4\pi r^2(\rho(r) - \rho(o)) = 2/\pi \int_0^\infty si(s) \sin rs \, ds$$

where $\rho(r)$ is electron density at vector r, $\rho(o)$ is average electron density, s is $4\pi \sin\theta/\lambda$, i(s) the interference function obtained by scaling to the calculated Compton scattering added to Σf_i^2 and then subtracting that combined term, Σf_i^2 is the average atomic scattering factor squared.

It is possible to recognise C-C and C-2nd C distances from such an RDF. However these are not especially useful except perhaps as a check that the procedure is satisfactory. C-3rd C and other conformationally sensitive peaks in this region can be further enhanced by deconvoluting the mean electron distribution about each of the atoms. Deconvolution is achieved by dividing the right hand side of the above equation by $(\Sigma f_i)^2$. Figure 2 (ref. 1) shows such an RDF weighted as r^2, in which C-3C and C-4C distances are clearly apparent as well as inter and intra molecular information at larger distances. The sharpening procedure, while useful, does tend to enhance spurious ripples associated with data termination. In fact, it is easy to be misled by such errors, especially when the RDF is calculated at

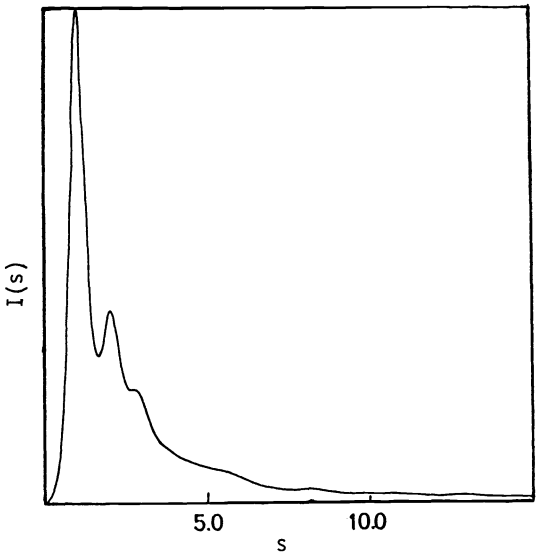

Fig. 1. WAXS from atactic PMMA

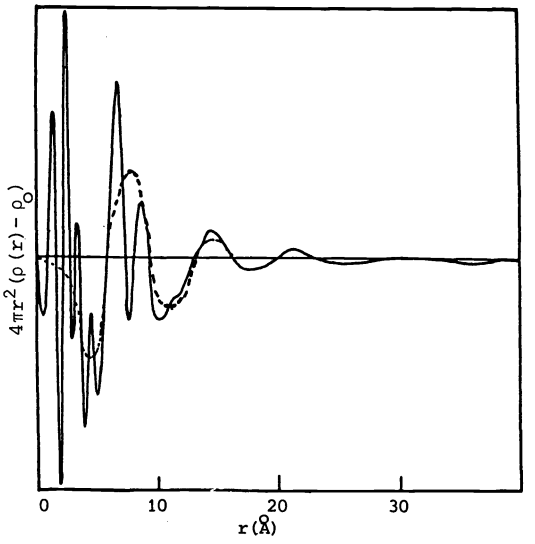

Fig. 2. RDF of atactic PMMA

intervals of r closer than $2\pi/s_{max}$ which is the resolution to which one is entitled. The method of sampled transforms introduced by Lovell et al. (ref. 2) is a useful discipline in the preparation of polymer RDFs and Fig. 2 (ref. 3) was generated in that way. The dashed curve of this figure outlines the damped ripple which is the interchain information derived from the first large peak of the data. The remaining information is essentially intramolecular and is in part superimposed on the intermolecular distances. RDFs can be useful, but they are but rearrangements of information, and in the case of polymers they have the additional drawback that while the inter and intra molecular maxima are often well separated on the scattering pattern, they are superimposed on the RDF. In the development below, the approach will be to keep the data in reciprocal space which will be the matrix for comparisons with scattering calculated by transforming conformational and packing models.

PMMA (ii) INFORMATION FROM ORIENTATION

In order to find which features of a scattering pattern are associated with correlations within a molecule, and which with correlations between, additional knowledge is necessary. Orientation of a glass by deformation leads to oriented diffraction patterns in which interchain features tend to concentrate on the equator and intra features on the meridian, as shown in Fig. 3 (ref. 4). For molecules which have pendulous side groups, the interpretation of oriented patterns may be more difficult, a point to which we will return when considering polystyrene below.

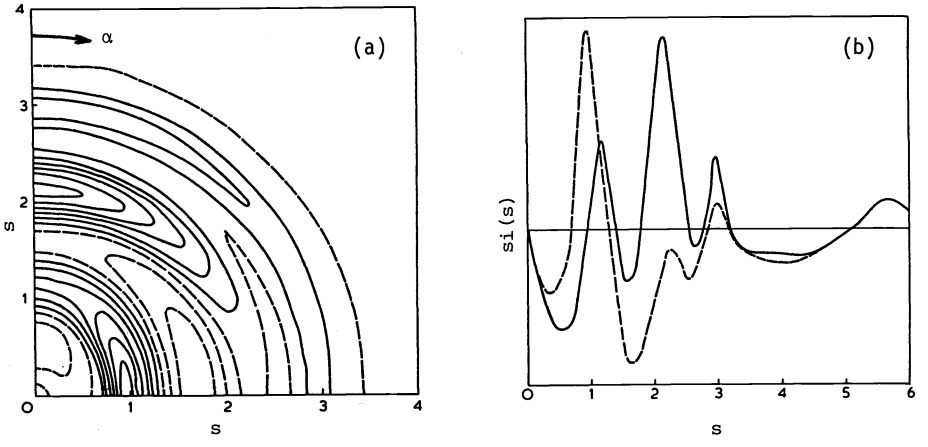

Fig. 3. (a) Quadrant of scattering, expressed as s i(s,α), from a sample of atactic PMMA oriented along the vertical axis. (b) Equatorial (dashed) and meridional (full) sections.

Orientation produces a wealth of additional information which can be interpreted on a number of levels, but first it is important to ask whether the orientation is itself changing the local conformation of the molecule. To a first approximation, the degrees of orientation which it is possible to introduce into the glass do not noticeably influence the local conformation. Figure 4 (ref. 5) illustrates this statement.

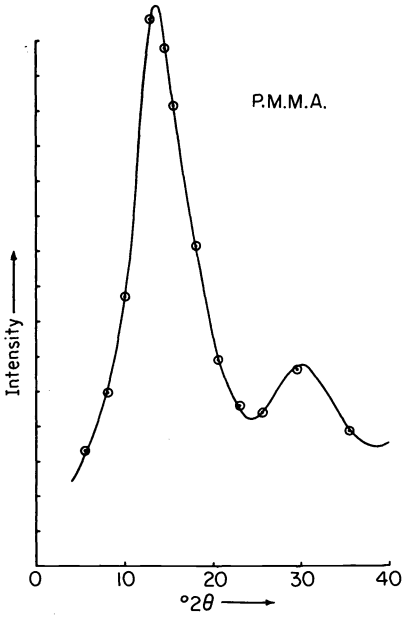

Fig. 4. Scattering from atactic PMMA. The intensity values (plotted as individual points) were obtained by azimuthally averaging the pattern of a two dimensional pattern with the appropriate sin α weighting function. The continuous curve is the scattering from an unoriented sample.

The three meridional peaks for atactic PMMA can be seen in the section in Fig. 3. The positions and relative intensities of these peaks are related to the conformation of the individual molecules.

PMMA (iii) SCATTERING CALCULATIONS

The strategy adopted to determine the conformation is to calculate the scattering from a PMMA molecule for a wide range of conformations. Initially attention is focussed on the conformations which are based on regular sequence of backbone bond rotation angles of the staggered type, and of these, only the sterically viable structures are considered further. The first calculations are for the syndiotactic molecule, the comparison being made with experimental data from syndiotactic PMMA glass which is very similar to that of the atactic material. Figure 5 shows a set of calculated curves for different conformations of the syndiotactic molecule, while the vertical dashed lines mark the position of the measured maxima. The sense of the rotation direction is defined oppositely for each of the two bonds of the racemic dyad of Fig. 6. The calculated curves show first and foremost that the scattering is sensitive to the molecular conformation. Comparisons indicate that the all trans (0,0,0,0) conformation is the most probable, where every other backbone bond angle, the one at the unsubstituted backbone carbon, is opened up to over 120° (122° was used for the first calculations). The next stage involves the refinement of the conformational parameters to optimise the match to experiment. For syndiotactic PMMA the best fit obtained for the conformation was: 10°, 10°, -10°, -10° (backbone rotation angles); 110°, 128° (backbone bond angles), and probably $\chi = 0°$ rather than 180° (angle of attachment of ester to backbone). Models have been built on the assumption that there is an underlying backbone conformation, which persists for a mean number of backbone bonds, and that the scattering observed will be equivalent to that calculated from such a sequence. Figure 7 shows the influence of sequence length on the calculated curves, the best fit corresponds to a run of 16-20 backbone bonds.

At this point we have a conformational model for syndiotactic PMMA. The scattering measured for the atactic material, which is reportedly 80% racemic (syndiotactic) dyads, is almost indistinguishable from that from the syndiotactic material. But perhaps more surprisingly scattering from the quenched isotactic glass is not particularly different either. The second and third meridional haloes are in much the same positions, although the first is very much weaker, if present at all. The conformation which gives the best calculated fit to data is based on the sequence of rotation angles 15,15,15,15, with all rotations being measured in

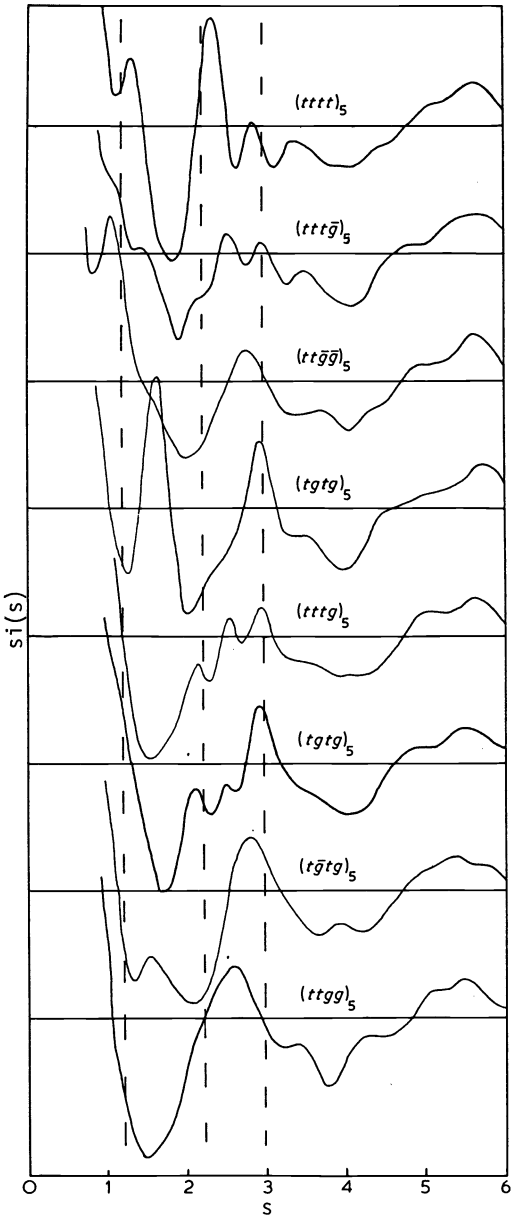

Fig. 5. Calculation of meridional scattering from single chain models of syndiotactic PMMA in different conformations. The model length in each case was 20 backbone bonds and the backbone bond angles 110° (α) and 122°. (Ref. 5). The vertical dashed lines mark the position of the observed meridional peaks for the quenched syndiotatic glass.

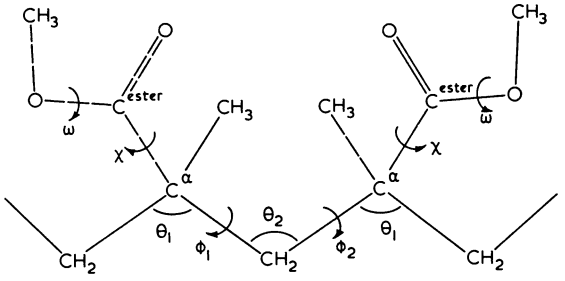

Fig. 6. Racemic dyad of syndiotactic PMMA drawn with rotation angles set to zero.

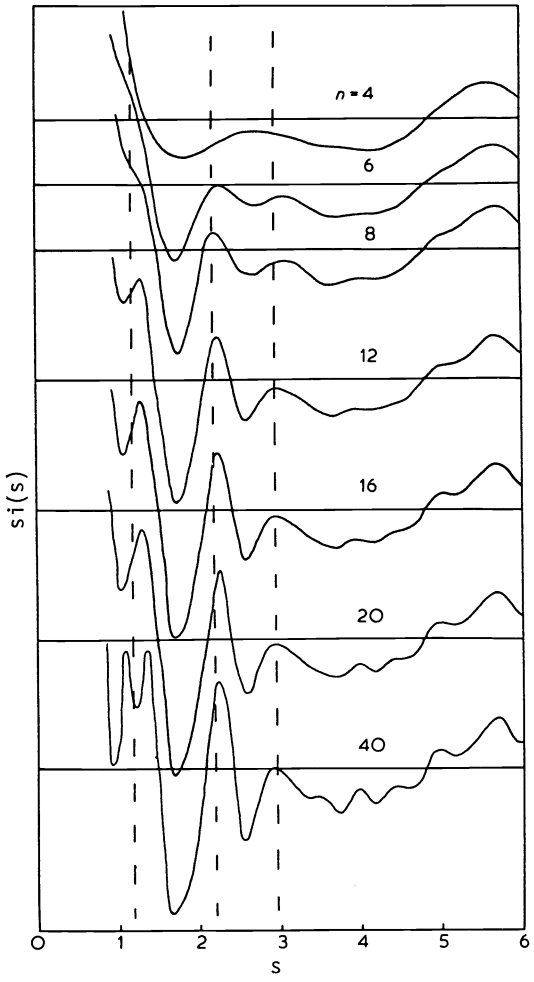

Fig. 7. Effect of increasing chain length for the proposed conformation (10°, 10°, -10°, -10°) $\theta_1 = 110°$, $\theta_2 = 128°$, n = number of backbone bonds.

the same sense. The distortion of the bond angles is similar to the syndiotactic molecule. It is apparent therefore, that as far as intra-chain scattering is concerned the local relative disposition of the side groups in space, which makes the major contribution to the observed scattering pattern is not greatly affected by tacticity. This finding is underlined by recent calculations of scattering (ref. 6) which were made for chains in which there was a statistical distribution of gauche bonds, and covering the full range of tacticities. Remarkably, for a probability of trans of 0.9 (≡ to the mean run length of 16-20), variations of tacticity over the whole range (using bond rotation parameters appropriate to syndiotactic) had very little influence on the scattering. Furthermore, for a racemic dyad fraction of 0.8, the change in trans probability from 0.8 to 1.0 affected the curves in the same way as using models of appropriate length in a single underlying conformation.

The conformation obtained for syndiotactic and quenched isotactic PMMA using this experimental analysis, confirm the conformational energy calculations of Sundararajan and Flory (ref. 5). Interestingly the syndiotactic molecule consists of sequences of bent segments and it is this shape which is probably responsible for the fact that syndiotactic material cannot be thermally crystallized, and it may even be an important factor in ensuring highly amorphous character of atactic PMMA which endows it with good optical clarity. The molecule of quenched isotactic PMMA is a slowly turning helix, although the position of the intermolecular peak indicates that the packing units are single rather than the double helices (ref. 7) predicted for the crystal structure (ref. 8).

PMMA (iv) USE OF HARMONIC FUNCTIONS IN THE ANALYSIS OF ORIENTED SCATTERING PATTERNS

The extra information available in the two-dimensional scattering from an oriented sample has been used so far in a rather high-handed way. It was critical in indicating which peaks were inter-molecular and which were intra-molecular and thus could be calculated from a model of a single molecule. However, a different analytical approach (refs. 9 and 10) has enabled the two-dimensional scattering to be properly handled. The scattering pattern is analyzed into spherical harmonics using the relation:

$$i_{2n}(s) = (4n + 1) \int_0^{\pi/2} i(s,\alpha)\, P_{2n}(\cos\alpha)\, \sin\alpha\, d\alpha$$

where P_{2n} are Legendre polynomials, and $i(s,\alpha)$ the experimental scattering.

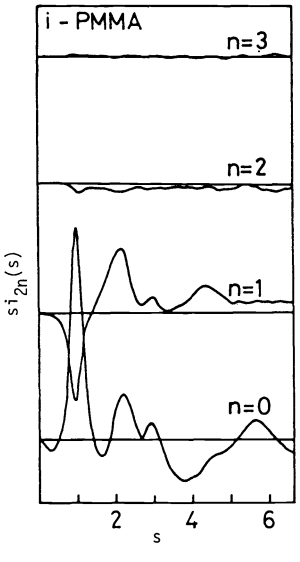

Fig. 8. $si_{2n}(s)$ curves for n = 0,1,2 and 3 derived from the experimental scattering from quenched isotactic PMMA. The vertical scale is the same for each component.

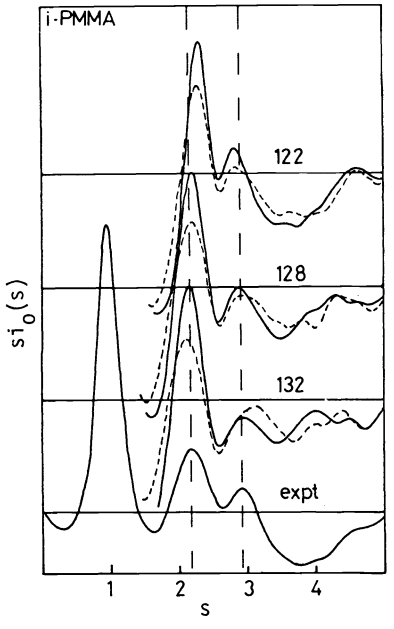

Fig. 9. Calculated $si_0(s)$ curves for the conformation (15°, 15°, 15°, 15°) and 20 backbone bonds. χ = 0° (—), 180° (---). The curves are drawn for different values of θ_2 (marked), θ_1 being set at 110°. The vertical dashed lines trace the positions of the meridional peaks in the experimental zero order harmonic curve drawn at the bottom. (ref. 10).

The experimental harmonics as a function of s are shown for quenched i-PMMA in Fig. 8. In $i_2(s)$ (n = 1) the meridional peaks correspond to maxima, the equatorial to minima. Their usefulness is illustrated by the question of the refinement of the distorted backbone bond angle. Figure 9 shows the $si_0(s)$ components for three possible pairs of bond angles. Figure 10 is $si_2(s)$, and Fig. 11 $i_4(s)$ for $\theta_2 = 122^o$ and 128^o only. In the last case experimental error is becoming significant and yet the difference between the predictions of the two models has become especially significant also. It is clear that of the two distorted bond angles $\theta_2 = 128^o$ is to be preferred. It is only on this point of detail the experimentally determined parameter is in conflict with that found from refined conformational energy calculations (ref. 5).

There is another aspect to the spherical harmonic analysis which is worthy of note. When an adequate match has been obtained with the scattering calculated from the model, then the ratio:

$$\frac{i_{2n}(s) \text{ experimental}}{i_{2n}(s) \text{ model}}$$

gives the series $P_{(2n)}$, which are the harmonic coefficients describing the degree of global orientation in the sample. This method of orientation measurement is particularly powerful, for not only does it give P_2 and higher coefficients (unlike the birefringence for example, which will only give P_2), but the model that is built defines the orienting unit.

POLYSTYRENE (PS)

PMMA might be described as a semi-rigid polymer, and certainly space filling models bear this out. The polystyrene molecule being singly substituted, is much more flexible as an isolated chain and yet it forms a polymer glass with a Tg similar to that of PMMA. Figure 12 shows the X-ray scattering from oriented atactic PS. The first maximum is equatorial as with PMMA and yet the peak is weaker and at a substantially lower angle. The second maximum is the

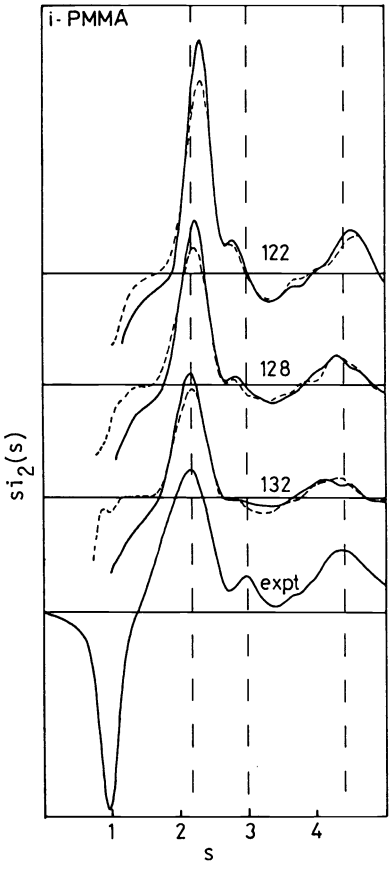

Fig. 10. Calculated $si_2(s)$ curves. Otherwise as Fig. 9 (ref. 10)

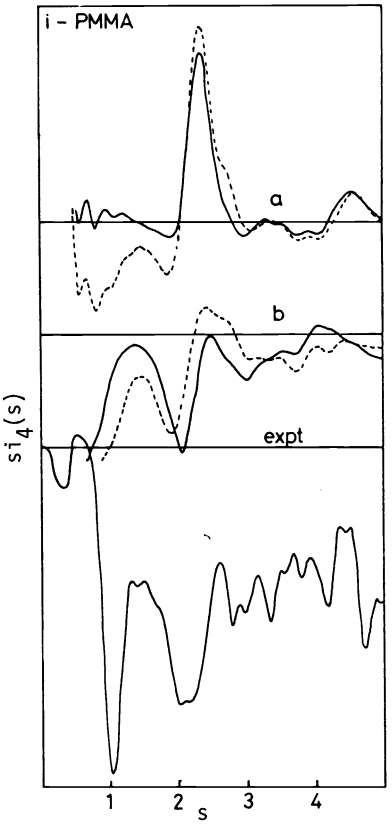

Fig. 11. Calculated $si_4(s)$ for the same model as in Figs. 9 and 10, but for $\theta_2 = 122^o$, (curve a) and 128^o (curve b) only. (ref. 10).

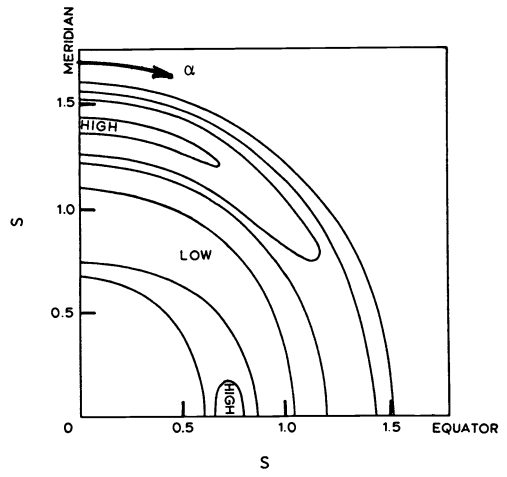

Fig. 12. Quadrant of scattering (as uncorrected intensity) from oriented atactic polystyrene.

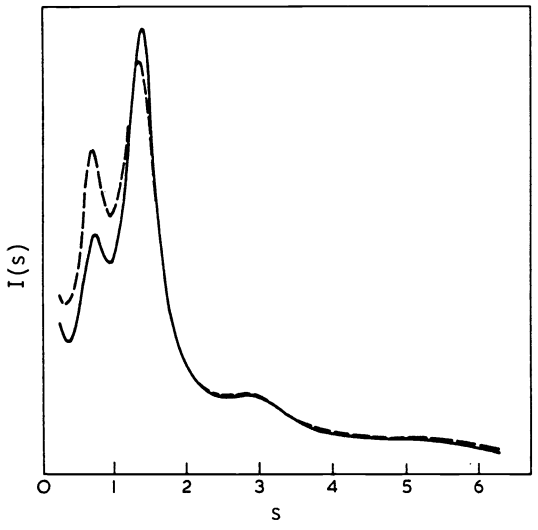

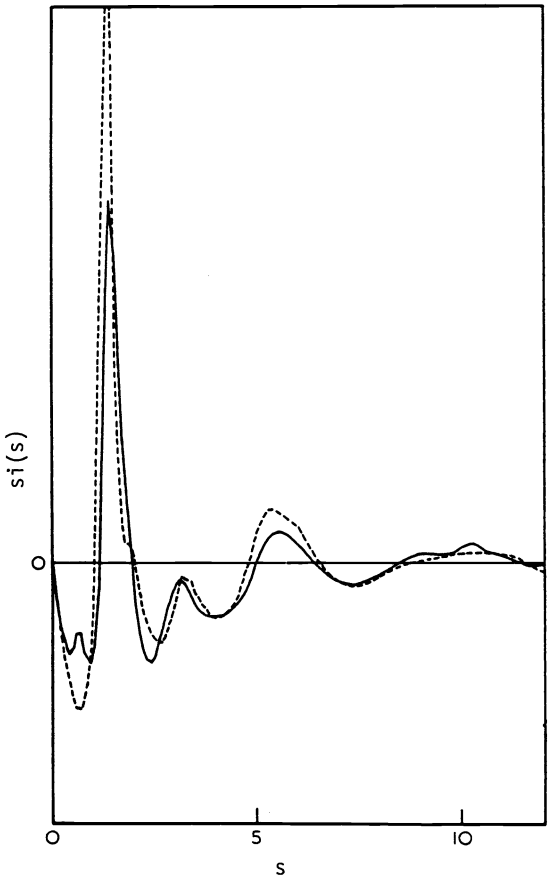

Fig. 13. The reduced intensity function si(s), for atactic PS (——) compared with that of liquid benzene (----) (ref. 11).

Fig. 14. The experimental scattering from an unoriented sample of atactic PS at 20°C (——) and 250°C (---).

most intense and it concentrates on the meridian. However, attempts to model the meridional scattering by calculations based on an isolated molecule have been unsuccessful. In fact the experimental scattering as a whole was closely similar to that for benzene (Fig. 13) (ref. 11). The only differences being the first equatorial maximum in the PS curve which is absent from the benzene scattering (and indeed from monomer styrene, and it has been called the polymerization ring (ref. 12)), and a small shoulder on the high angle side of the main intermolecular peak from benzene which is absent from the PS curve. This small shoulder has been ascribed to special benzene ring correlations and it will be discussed in a different context below. We have concluded (ref. 13) that the main meridional maximum corresponds to correlations between phenyl groups which may not belong to the same molecule, and one needs to focus on the first equatorial maximum to give information on the chain packing. This peak however shows a striking increase in intensity with increasing temperature, Fig. 14. This behaviour, coupled with the unusually low angle of the peak, bearing in mind the polymer density and likely range of chain repeat distances per chemical repeat, indicates that the phenyl groups of adjacent molecules organise themselves into loose stacks, and it is the contrast between the stacks (2 polymer chains/stack), rather than individual molecules which account for the peak. Its increase with temperature is associated with the fact that it is actually an electron deficient region along the core of the stack which gives the scattering contrast. It is the core, increasing substantially in area to accomodate thermal expansion, which enhances the scattering intensity. The model thus involves the microsegregation of the phenyl groups which interpenetrate in groups. The increasing intensity of the chain peak with temperature is accounted for by an electron deficient region at the centre of the

phenyl groups, while the fact that the peak concentrates onto the equator in the oriented sample demonstrates that the microsegregated phenyls arrange themselves as stacks. The fact that the relative disposition of phenyls is controlled to some extent by their packing with other similar groups from neighbouring chains, in addition to the conformation of the backbone to which they are attached, means that measurement of this disposition by WAXS cannot give an accurate indication of the backbone conformation. There is no evidence that the conformation is anything but random. The tendency of the phenyl groups to segregate is also clearly seen in the crystal structure of i-PS (ref. 14), where the phenyl groups are arranged in stacks, each of which is associated with six surrounding backbones in the 3/1 helical conformation. It has also recently been noted that the 110 peak in the scattering from the isotactic crystal increases markedly in intensity with increasing temperature (ref. 15).

POLYCARBONATE (PC): AN EXAMPLE OF A GLASSY POLYMER WITH AROMATIC GROUPS IN THE BACKBONE

Figure 15 shows the scattering from an oriented sample of polycarbonate (ref. 16). It is helpful to consider two particular features of this plot; the first is the small shoulder on the high angle side of the main interchain peak at $s \simeq 1.9\text{Å}^{-1}$, the second the small peak at $s \simeq 0.5\text{Å}^{-1}$. The shoulder at $s \simeq 1.9\text{Å}^{-1}$ is particularly interesting as it appears more or less distinctly in many main chain aromatic polymers. Figure 16 shows a selection of curves from unoriented samples of this type of polymer (ref. 17). Furthermore, as mentioned above, the 1.9Å^{-1} feature is also apparent in the scattering from liquid benzene, where it is interpreted as representing special, possibly face-face, correlations between phenyl rings. In oriented patterns the small peak does not distinctly intensify on either the meridian or equator and for PC, it is if anything more intense at $\alpha \simeq 45^{\circ}$. This angle is not known with any precision, and yet it is in line with the likely conformation of the polycarbonate chain in which the virtual bonds will make an angle of 30-35° with the local chain axis. It appears therefore that as in liquid benzene there are special local correlations between the aromatic rings of neighbouring chains. Again one should draw attention to PS in which there is no sub-peak on the high angle side of the main interphenyl maximum, it is possible that its absence is indicative of a different form of special packing within the phenyl stacks of this polymer.

The small maximum at $s = 0.7\text{Å}^{-1}$ is a particular feature of the scattering from polycarbonate. In oriented samples it concentrates clearly onto the meridian and its position correlates with the structural repeat of the chain in a near to extended conformation. That such a peak is apparent is not surprising in itself, although its behaviour on annealing is particularly interesting especially in light of the well known changes in mechanical properties of polycarbonate induced by sub-Tg heat treatments (ref. 18).

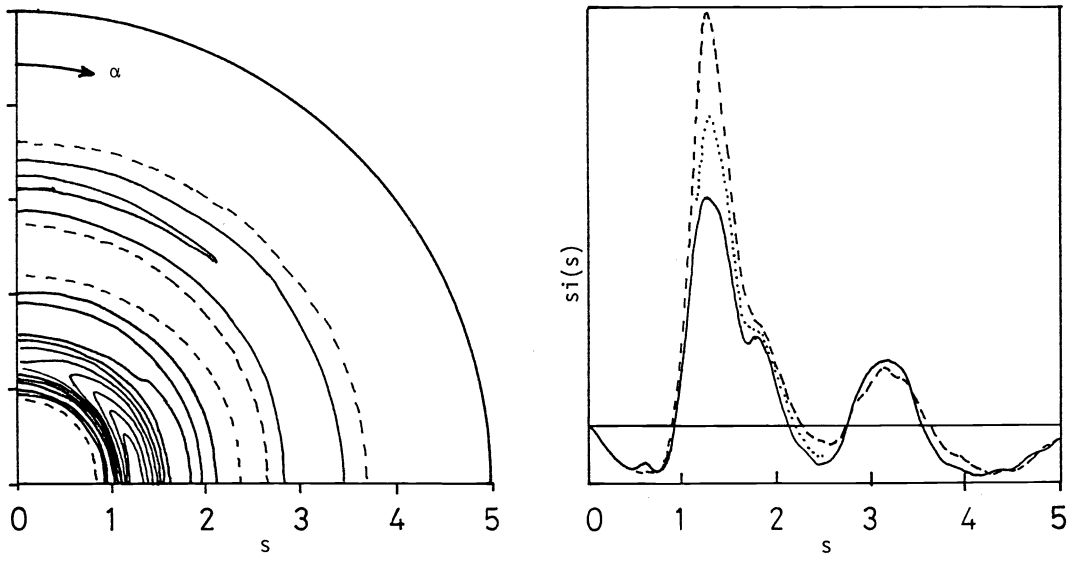

Fig. 15. The experimental scattering expressed as si(s,α) for a sample of glassy polycarbonate oriented about the vertical axis. The sections in the right hand plot are equatorial (---), meridional (——) and at 45° to the extrusion axis (···).

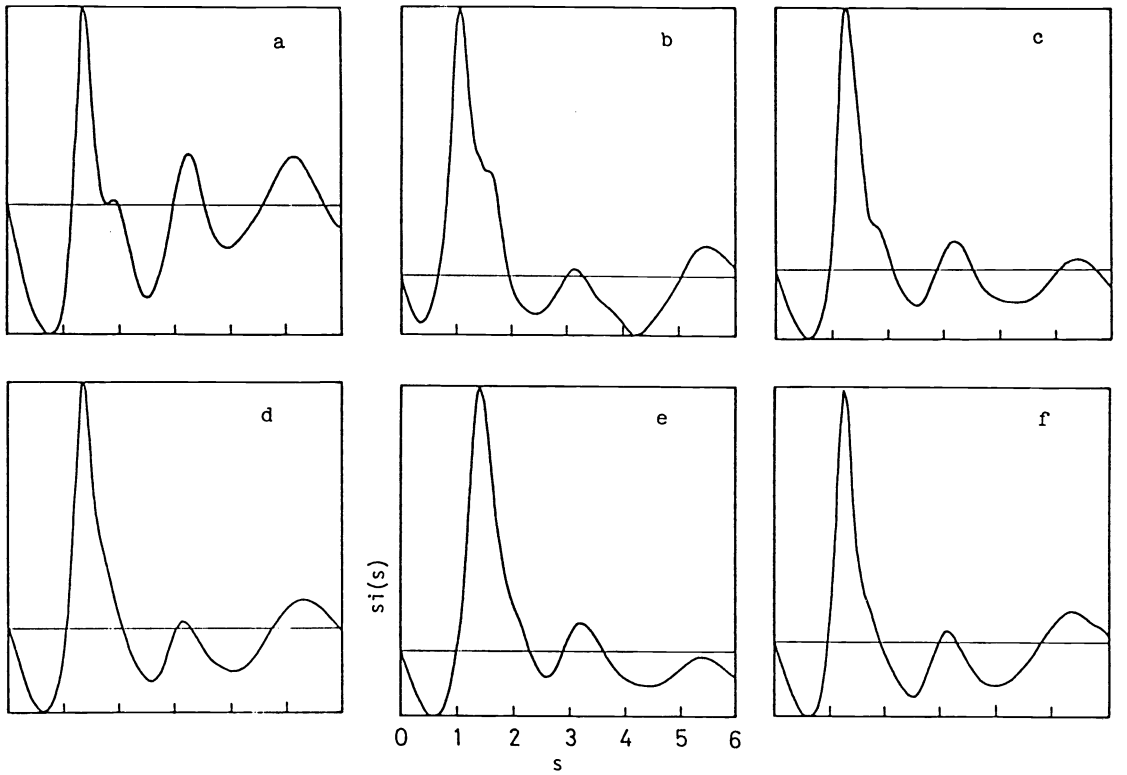

Fig. 16. The scattering measured from a range of glassy polymers with phenyl groups in their backbones (ref. 17). a) poly p-phenylene sulphide; b) poly 2-6 dimethyl p-phenylene oxide; c) polycarbonate; d) polyether sulphone; e) polyether ether ketone; f) poly sulfone

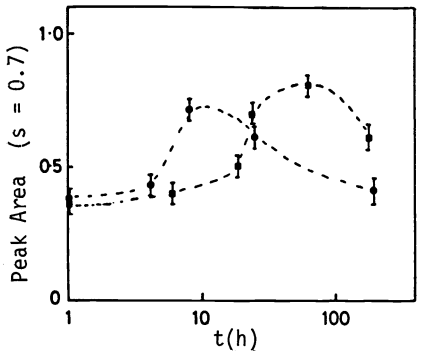

Fig. 17. Plot of the area of the intra-chain peak at $s \sim 0.7\text{Å}^{-1}$ as a function of annealing time at 120°C (■) and at 130°C (●).

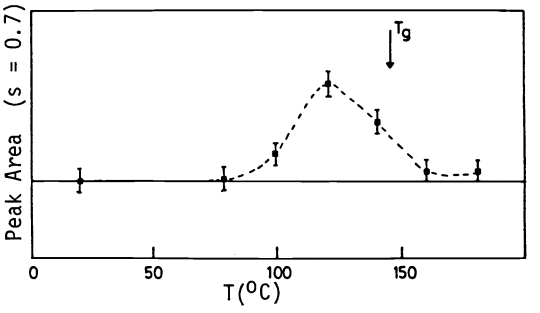

Fig. 18. Area of intra-chain peak at $s \sim 0.7\text{Å}^{-1}$ as a function of temperature for 24h anneals.

Figure 17 shows the variation of peak area with annealing time at two temperatures below Tg. It increases to a maximum and then decreases again. This has been interpreted as demonstrating the nesting of the butterfly conformation associated with the carbonate groups as these units on adjacent chains develop the appropriate register and interlock. The decrease at longer times is not as easy to understand. It has been proposed that a second layer of chain correlation develops, with the same c/2 stagger seen in the crystal structure, and eliminates the peak. (c = chemical repeat.) The results of Fig. 18 show that there is no increase in peak area above Tg. At first sight this could be ascribed to the 'overaged' state at the higher temperatures. However, no increase was observed after short anneals, and a sample annealed above Tg when cooled and given a sub-Tg treatment developed the enhanced peak area in line with Figure 17. We are thus faced with evidence that the special local correlations developed by heat treating the glass and associated with nesting of adjacent units in the butterfly conformation melt out, in the first order meaning of the term, at Tg. Such behaviour may well be associated with the double maxima severally reported in DSC traces of polycarbonate (ref. 19).

LIQUID CRYSTALLINE POLYMERS

The thermotropic liquid crystalline polymer which will be the focus of interest here is a random copolyester of hydroxy naphthoic and hydroxy benzoic acids. High degrees of molecular alignment are readily achieved in these polymers with modest flow fields, and the scattering from such a sample is shown in fig. 19. The meridional scattering consists of maxima at approximately s = 1,2,3,4$\mathring{A}^{-1}$ with that at 3$\mathring{A}^{-1}$ being the most intense. It is possible to model the positions of these peaks (ref. 20,21) in terms of a one dimensional lattice model based on two repeats, equivalent to the lengths of the benzoic and naphthoic moieties, arranged at random. The intensity and sharpness of the 3$\mathring{A}^{-1}$ peak can be understood as the near coherence of the 3rd order harmonic of the benzoic repeat and the 4th order of the naphthoic. The molecular transforms of either unit also tend to enhance the intensity in the region of s = 3. An important aspect of the successful modelling of these maxima is that the copolymer is confirmed as being random. Figure 20 shows the comparisons of the experimental intensity distribution along the meridian, of a fibre sample having proportions of HBA/HNA of 70/30, with the random model prediction and the prediction of a 'blocky' model in which like units were arranged in runs of 10.

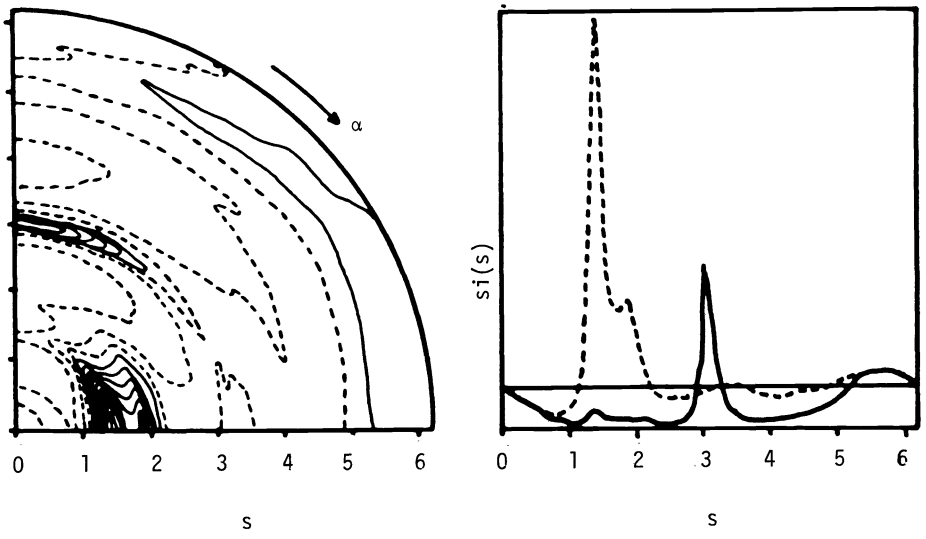

Fig. 19. WAXS scattering from an extruded sample of a random thermotropic copolyester based on hydroxy benzoic and naphthoic acids. Sections: equatorial (----), meridional (——).

There is a considerable quantity of information in the scattering data of fig. 19, but here attention will be given to two features which, rather than attest to the uniqueness of the liquid crystalline state, provide an interesting link with the polycarbonate pattern considered in the previous section. Firstly, the sub-peak at s = 1.9$\mathring{A}^{-1}$ on the high angle side of the main equatorial interchain maximum is present in the scattering from the thermotropic co-polyester as it was with the flexible polymers having phenyl groups in the backbone. In the liquid crystalline case the sub-peak is clearly defined and the well oriented diagram shows that it concentrates close to the equator but not on it. The angular divergence from the equator is about 12°, and a useful comparison can be made with the angles the virtual bonds in the homopolymers in trans conformation will make with the chain axis.

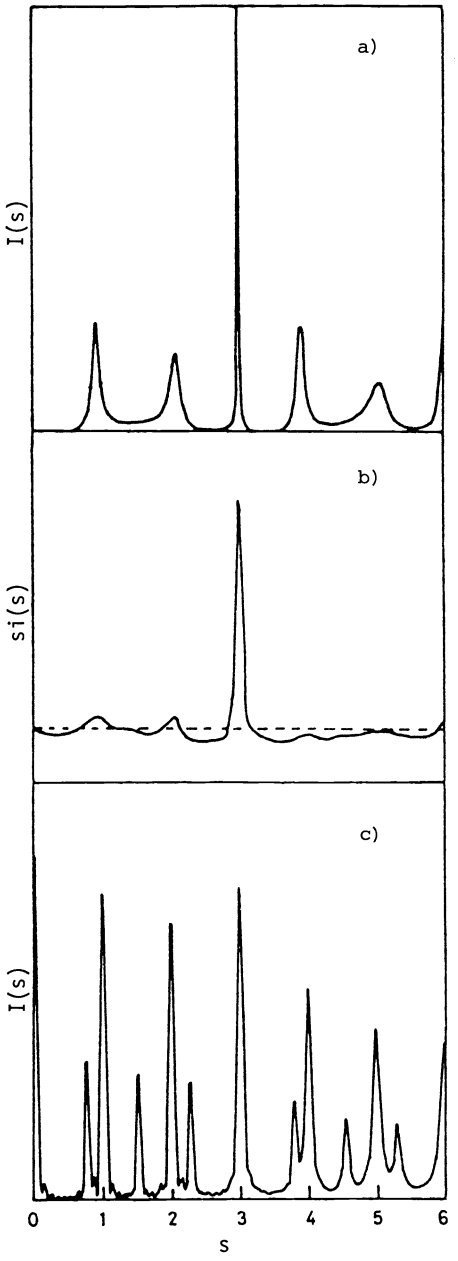

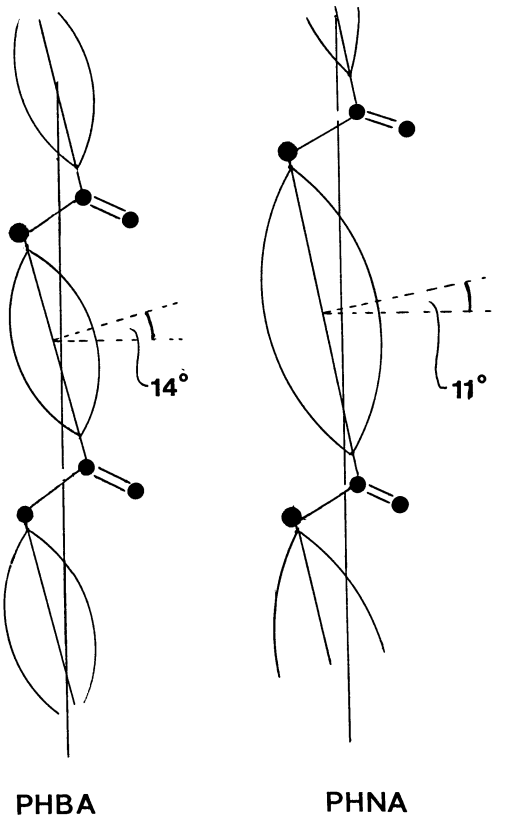

Fig. 21. Schematic diagram showing the angles made by the virtual bonds for molecules of poly HBA and HNA in the trans conformation.

Fig. 20. a) Calculated meridional intensity for a point model corresponding to a 70/30, HBA/HNA random copolymer sample, b) Measured intensity from a fibre, c) Calculated intensity for the case where like units are grouped in runs of 10.

The angles are shown schematically, in terms of the normal to the plane of the aromatic groups in fig. 21. The other aspect which is perhaps similar to the polycarbonate case is the influence of annealing on the first meridional maximum, that close to s = 1Å^{-1}. Figure 22 shows that when a well oriented fibre is annealed close to the melting point, the peak laterally concentrates onto the meridian and increases in intensity. Its position along the meridian is in accord with the randomness of the copolymer, and yet the lateral concentration demonstrates the development of longitudinal register between the latterally arranged chains. The fact that this register is achieved between random molecules and that there is no other sampling on the layer, has lead to the proposal that the register is achieved between random but similar sequences in the adjacent chains (ref. 22).

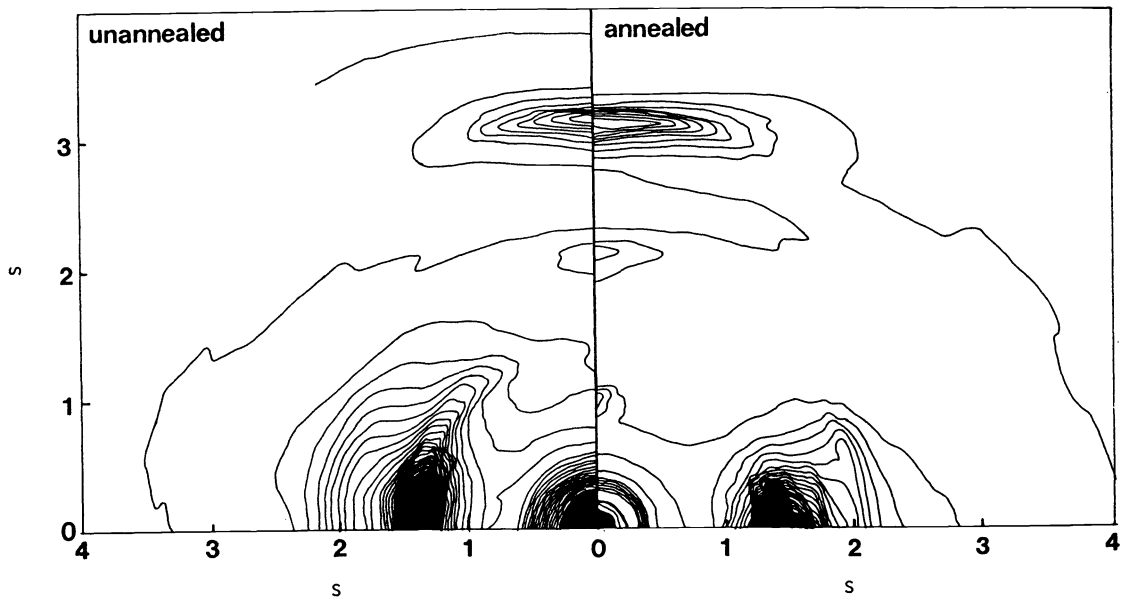

Fig. 22. Scattering from fibres before and after annealing. The concentration of intensity onto the meridian at $s \simeq 1\text{Å}^{-1}$ is apparent in the annealed pattern.

FINALE

Over the past ten years the technique of WAXS analysis has provided support for the picture that in glasses and melts of flexible polymer the molecule follows a random trajectory as it would in a θ solvent. In particular, it was able to eliminate the fold modified meander model for molten polyethylene (ref. 23). The resolution of wide angle methods enables them to explore the interaction of neighbouring chains. While there are no special correlations apparent in either polyethylene or PMMA, the presence of phenyl groups, whether in the backbone as in polycarbonate or as side groups as in polystyrene, lead to special interchain features in the scattering. In oriented systems showing liquid crystalline order, the patterns are not only sharper, reflecting the long range orientation correlations, but show levels of positional order which reflect the chemical make-up of the rigid molecule.

Much remains to be done, the application of WAXS to molecular series in which the chemistry is changed systematically will provide further insight into the rules that govern the packing of the macromolecular motif; while the development of wide angle neutron scattering of selectively deuterated molecules will open fresh vistas for our understanding.

REFERENCES

1. G.R. Mitchell and A.H. Windle, J. Appl. Cryst., 13, 135-140 (1980).
2. R. Lovell, G.R. Mitchell and A.H. Windle, Acta Cryst., A35, 598-603 (1979).
3. J.R. Waring, R. Lovell, G.R. Mitchell and A.H. Windle, J. Mat. Sci., 17, 1171-1186 (1982).
4. R. Lovell and A.H. Windle, Polymer, 22, 175-184 (1979).
5. P.R. Sundararajan and P.J. Flory, J. Amer. Chem. Soc., 96, 5025 (1974).
6. G.R. Mitchell, Ph.D thesis, Cambridge, 1983.
7. R. Lovell and A.H. Windle, Macromolecules, 14, 211-212 (1981).
8. H. Kusanagi, H. Tadokoro and Y. Chatani, Macromolecules, 9, 531-532 (1976).
9. G.R. Mitchell and R. Lovell, Acta Cryst., A37, 189 (1981).
10. G.R. Mitchell and A.H. Windle, Colloid and Polymer Sci., 260, 754-761 (1982).
11. A.H. Narten, J. Chem. Phys., 67, 2102 (1977).
12. J.R. Katz, Trans. Faraday Soc., 32, 77 (1936).
13. G.R. Mitchell and A.H. Windle, Polymer, 25, 906-920 (1984)
14. G. Natta, P. Corradini, I.W. Bassi, Nuovo Cimento Suppl., 15, 68 (1960).
15. D. Sadler, recent communication.
16. G.R. Mitchell and A.H. Windle, Colloid and Polymer Sci., 263, 280-285 (1985).
17. T.P.H. Jones, Ph.D thesis, Cambridge 1983.
18. J.H. Golden, B.L. Hammant and E.A. Hazell, J. Appl. Polymer Sci., 11, 1571 (1967).
19. K. Neki and P.H. Geil, J. Macromol. Sci. Phys., B8, 295 (1973).
20. R.A. Chivers, J. Blackwell and G.A. Gutierrez, Polymer, 25, 435 (1984).
21. G.R. Mitchell and A.H. Windle, Colloid and Polymer Sci., 263, 230-244 (1985).
22. A.H. Windle, C. Viney, R. Golombok, A.M. Donald and G.R. Mitchell, Faraday Discussions of the Chemical Soc., 79, paper 5 (1985).
23. R. Lovell, G.R. Mitchell and A.H. Windle, Faraday Discussions, 68, 114-115 (1979).